Effect of surface roughness on hydraulic loss in spiral case

TAKASHI KUBOTA, and YUJI TAKAMI
Dept of Mech. Eng., Kanagawa University, Yokohama, Japan
FENGQIN HAN
Huazhong University of Science and Technology, Wuhan, P.R.China
FRANCOIS AVELLAN
IMHEF-EPFL, Lausanne, Switzerland

ABSTRACT

The increment of frictional deficiency by roughening the inner wall of spiral case is extracted from the optimum specific hydraulic energy deficiencies of a model Francis turbine that was measured by changing surface roughness of the spiral case. Assuming the free vortex flow in the spiral case, the frictional deficiency is predicted for the smooth and roughened spiral cases. By comparing the predicted deficiency with the measured increment of deficiency due to the roughness increase, the admissible roughness for the spiral case and the roughness conversion coefficient from the arithmetic mean roughness to the equivalent sand roughness are investigated.

Introduction

The surface roughness of the components in hydraulic turbines may affect the friction loss and the hydraulic performances, if the roughness exceeds the admissible roughness under the given Reynolds number. There is a little paper, so far, that systematically investigates the effect of the surface roughness of the various components in hydraulic turbines. To investigate the effect of surface roughness on the hydraulic performance of a Francis turbine, a series of model tests was executed in IMHEF, EPFL under the test heads of 10 and 5 m with changing the roughness of spiral case, stay vanes/guide vanes, runner and draft tube in the order[1].

This paper tries to extract the optimum energy efficiency η_{Eopt} from the measured hydraulic efficiency η_h for both the smooth and roughened spiral cases. Then, the effect of the roughness in the spiral case on the optimum energy deficiency δ_{Eopt} (=1.0 - η_{Eopt}) is evaluated carefully. Assuming the free vortex flow in the spiral case, the frictional deficiency is predicted along a representative stream line for the smooth and roughened spiral cases. By comparing the predicted deficiency with the measured increment of deficiency due to the roughness increase in the spiral

case, the admissible roughness for the spiral case and the roughness conversion coefficient from the arithmetic mean roughness to the equivalent sand roughness is investigated.

Frictional deficiency obtained with model tests

Model turbine and surface roughness

The tested model Francis turbine has the reference radius R_{ref} of 0.200 m at runner outlet. The test Reynolds number was changed by executing the performance measurements under the test heads of 10 m and 5 m. With the model turbine having the hydraulically smooth surfaces of 0.3 to 0.5 Ra from the spiral case inlet to the draft tube outlet, the hydraulic performance characteristics of discharge coefficient ϕ, specific hydraulic energy coefficient of turbine ψ, output power coefficient Π and hydraulic efficiency η_h were measured as a reference data. It is called as the all-smooth test. Then the only spiral case was roughened to 5 Ra. The hydraulic performances with the roughened-case tests were successively measured to evaluate the roughness effect of the spiral case[1].

Hydraulic characteristics of tested model

As an example of a series of the test results with the different surface roughness, Fig. 1 shows the characteristic diagram of the specific hydraulic energy coefficient ψ versus the discharge coefficient ϕ for the roughened-case test at the various guide vane angles from 12.5 to 32.5 degrees under the test head of 10 m. Similarly, Fig. 2 and 3 illustrate the diagrams of hydraulic efficiency η_h versus ϕ, and η_h versus ψ, respectively. The diagrams with other tests show similar tendency. Among the measured hydraulic characteristics, the energy coefficient ψ, discharge coefficient ϕ, output power coefficient Π and hydraulic efficiency η_h are calculated with the following equations;

$$\psi = \frac{2E}{\left(\omega R_{ref}\right)^2} \tag{1}$$

$$\phi = \frac{Q/\pi R_{ref}^{\ 2}}{\omega R_{ref}} \tag{2}$$

$$\Pi = \frac{2P}{\rho\pi\omega^3 R_{ref}{}^5} \tag{3}$$

$$\eta_h = \frac{\omega T}{\rho Q E} \tag{4}$$

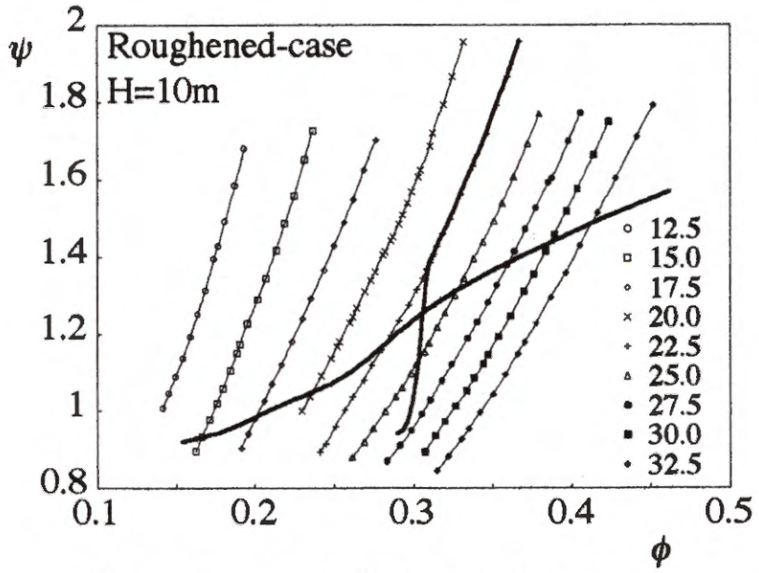

Fig. 1 Energy vs discharge characteristics

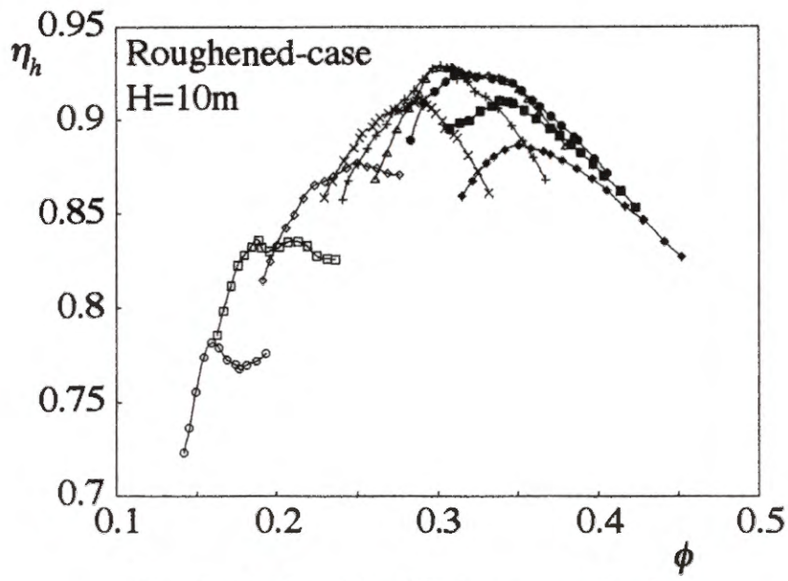

Fig. 2 Hydraulic efficiency vs discharge characteristics

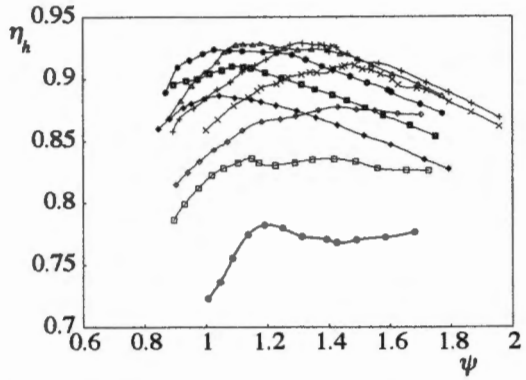

Fig. 3 Hydraulic efficiency vs energy characteristics

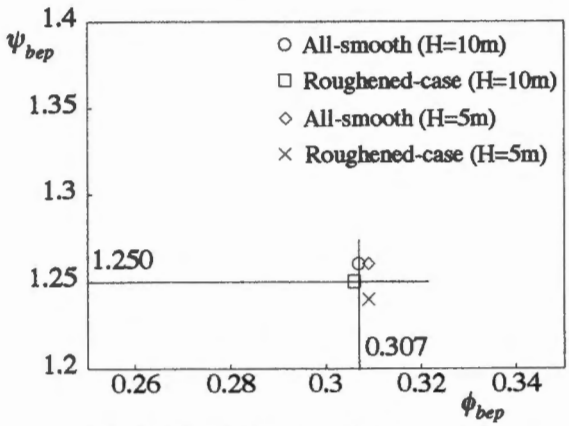

Fig. 4 Best efficiency point ψ_{bep} and ϕ_{bep}

where E (J/kg) is the specific hydraulic energy of the turbine, ω (rad/s) the angular speed of rotation, Q (m^3/s) the turbine discharge, P (W) the runner output power and ρ (kg/m^3) the density of water, respectively.

Surface roughness and best efficiency point

The best efficiency operating points ψ_{bep} and ϕ_{bep} for the respective tests are

collectively shown in Fig. 4 under the test heads of 10 m and 5 m. The roughness of spiral case does not affect the ψ_{bep} and ϕ_{bep} within the measured inaccuracy. The representative best efficiency coefficients ψ_{bep} and ϕ_{bep} are selected as 1.25 and 0.307, respectively.

Energy deficiency obtained with model tests

To find the increment of energy deficiency with the surface roughness of the spiral case, the specific hydraulic energy deficiency δ_E has to be analyzed from the above measured characteristic diagrams. Since the discharge specific speed n_{sQ} is computed as 74.0 at the representative best efficiency point, the best discharge efficiency η_{Qbep} and the power efficiency η_{Rbep} can be estimated according to the Ref.(2). The discharge and power efficiencies η_Q and η_R at an arbitrary test point can be calculated with the η_{Qbep} and η_{Rbep} by assuming that the leakage discharge coefficient ϕ_L and the disc/cylindrical friction power coefficient Π_L are constant irrespective of operating points as follows;

$$(1-\eta_Q)\phi = (1-\eta_{Qbep})\phi_{bep} \tag{5}$$

$$(1-\eta_R)\frac{\Pi}{\eta_R} = (1-\eta_{Rbep})\frac{\Pi_{bep}}{\eta_{Rbep}} \tag{6}$$

The energy efficiency η_E can be computed from the measured hydraulic efficiency η_h by using the above η_Q and η_R with the following equation;

$$\eta_E = \frac{\eta_h}{\eta_Q \eta_R} \tag{7}$$

Finally, the energy deficiency δ_E can be determined at an arbitrary test point as follows;

$$\delta_E = 1 - \eta_E \tag{8}$$

Incidentally, the runner energy coefficient ψ_R and the runner discharge coefficient ϕ_R at an arbitrary operating point can be obtained from the measured ψ and ϕ by the following equations;

$$\psi_R = \eta_E \psi \tag{9}$$

$$\phi_R = \eta_Q \phi \tag{10}$$

Extraction of optimum energy deficiency

As an example of the runner characteristic diagrams of η_E - ϕ_R thus obtained, Fig. 5 shows the energy efficiency characteristics with the roughened-case under the test head of 10 m. An envelope curve of $\eta_{Eenv\phi}$ - ϕ_R can be drawn that comes in contact with the various η_E-ϕ_R curves for the different guide vane openings. The bold curve from the lower left to the upper right in Fig. 1 corresponds to the envelope curve that is the optimum operating condition with changing discharge in Fig. 5.

By plotting a new curve of energy deficiency (with ϕ basis) $\delta_{Eenv\phi}$ =1 - $\eta_{Eenv\phi}$ versus the square of runner discharge ϕ_R^2 corresponding to the above envelope curve as shown in Fig. 6, a tangential straight line $\delta_{Etan\phi}$ to the deficiency curve can be drawn through the origin of the diagram. The tangential point determines the optimum discharge ϕ_{Ro} and its deficiency $\delta_{Eo\phi}$[3].

Similarly, the optimum runner specific hydraulic energy ψ_{Ro} and its $\delta_{Eo\psi}$ can be determined based on the envelope curve to the η_E versus ψ_R[3]. As imagined from Fig. 3, however, the number of η_E versus ψ_R curves to be enveloped is smaller especially in the higher ψ_R region. Therefore, the optimum deficiency $\delta_{Eo\psi}$ based on the ψ_R seems to be for reference only. The nearly vertical bold line in Fig. 1 corresponds to the optimum operating condition with changing runner energy ψ_R.

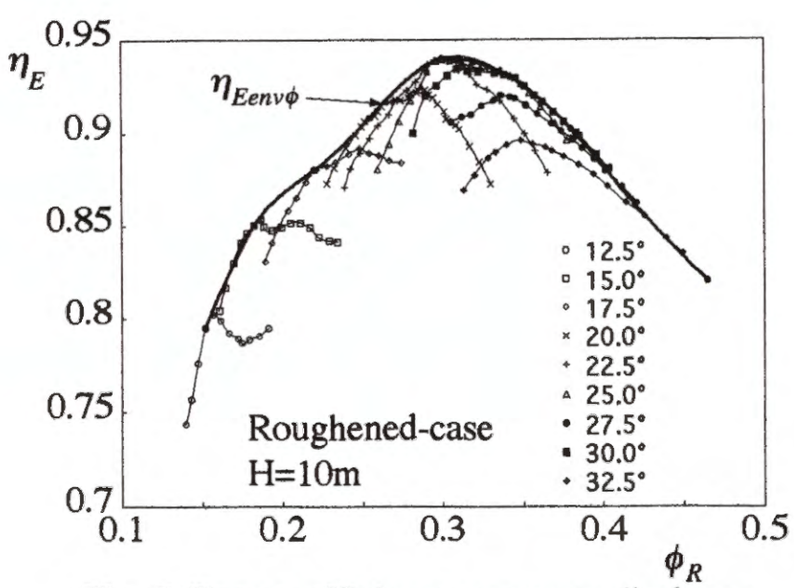

Fig. 5 Energy efficiency vs runner discharge

Effect of spiral case roughness on optimum energy deficiency δ_{Eo}

The optimum deficiency δ_{Eo} extracted in Fig. 6 is proportional to the square of discharge only, and does not include the deficiency that is out of proportion to the discharge such as the runner shock loss and swirl loss, etc. It is, therefore, preferable to investigate the variation of frictional deficiency i.e. the effect of roughness. The increment in the optimum deficiency between the $\delta_{Eo\text{-}rough}$ obtained with the roughened case and the $\delta_{Eo\text{-}smooth}$ obtained with the all smooth components, $\Delta\delta_{Eo} = \delta_{Eo\text{-}rough} - \delta_{Eo\text{-}smooth}$ can be evaluated as the increase of friction deficiency by roughening the spiral case.

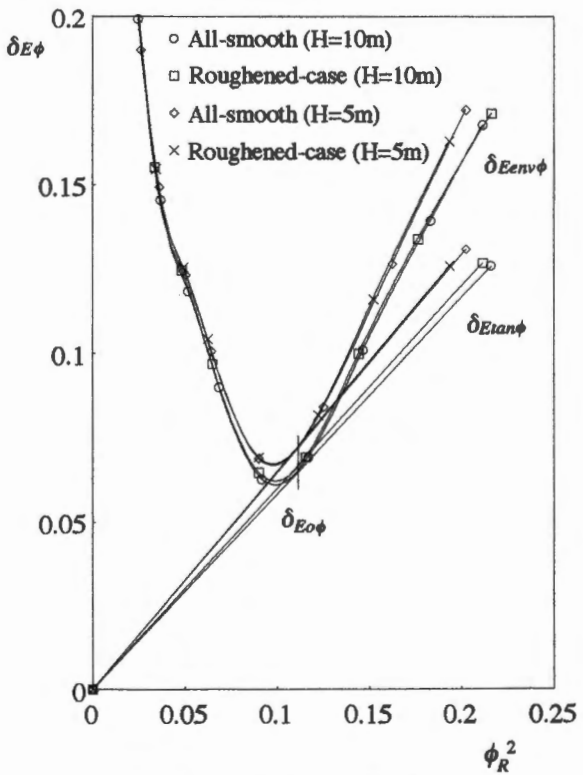

Fig. 6 Optimum energy deficiency

The extracted optimum specific hydraulic energy deficiency and the increment of deficiency due to the roughness increase are summarized in Table 1. The extracted optimum deficiencies amount the values from 5.7 to 6.3 % of the test head for the model turbine with all smooth components. Comparing the test head of 10 m and 5 m under the ϕ basis, the deficiency under the lower head is higher irrespective of roughness conditions. It is also confirmed that the optimum deficiency of the roughened case is higher than that of the smooth case by 0.1 % at the higher head of 10 m under the ϕ basis. On the other hand, there is actually no incremental deficiency due to the roughness increase under the lower head of 5 m.
Under the ψ basis, the qualitative tendency of the deficiency is similar, however, the quantity of incremental deficiency of 0.3 % is very large. Because of the reason that was mentioned above, the values under the ϕ basis will be analyzed mainly.

Table 1 Optimum specific hydraulic energy deficiency and increment of deficiency

Head (m)	Base	δ_{hr} of All smooth	δ_{hr} of Roughened case	Increment of δ_{hr} by roughness
10	ϕ	0.0571	0.0582	0.0011
10	ψ	0.0583	0.0617	0.0034
5	ϕ	0.0630	0.0635	0.0005
5	ψ	0.0623	0.0653	0.0030

Frictional deficiency obtained numerically

Velocity distribution in spiral case

The shape of spiral case used is shown in Fig. 7 having the inlet diameter D_3 of 0.474 m. Figure 8 shows the distribution of meridional cross sectional area (non-dimensioned with the inlet area A_{sin}) around the circumferential angle θ (starting at the inlet of nose stay vane). The case has the non-circular cross section at the end of spiral, therefore, the area decreases rapidly at the angle larger than 330 degs.

Assuming the flow of free vortex in the case, the center (representative) stream-line can be obtained by finding the vertical line that divide the discharge in half in the respective cross sections of the spiral case as shown in Fig. 7.

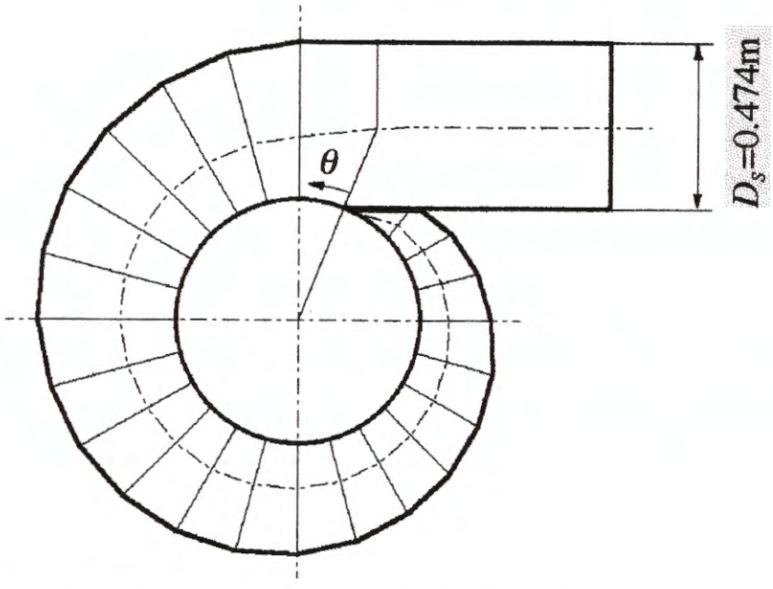

Fig. 7 Spiral case and representative stream line

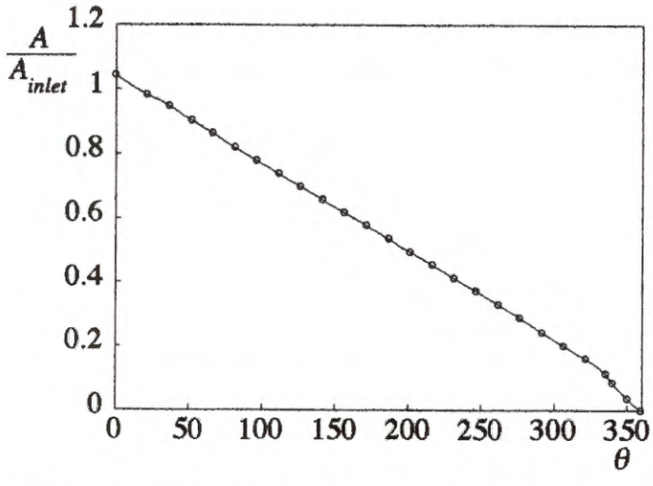

Fig. 8 Distribution of cross sectional area vs circumferential angle

The representative velocity along the center stream-line V_{center} is obtained by assuming the constant circulation around the spiral in that the product of circumferential velocity component $V_{\theta\text{-}center}$ and the radius from the center of runner shaft is conserved. The radially inward velocity component $V_{r\text{-}center}$ at an arbitrary

angle can be obtained from the relevant angle θ_S as follows;

$$V_{r-center} = V_{\theta-center} \tan\theta_S \tag{11}$$

The velocity along the representative stream-line can be determined with the following equation;

$$V_{center} = \sqrt{V_{\theta-center}^{\ 2} + V_{r-center}^{\ 2}} \tag{12}$$

The distribution of the representative velocity (non-dimensioned with the inlet velocity V_{inlet}) around the circumferential angle is shown in Fig. 9. The velocity increases with the angle up to the 1.6 times of the inlet velocity at the spiral end.

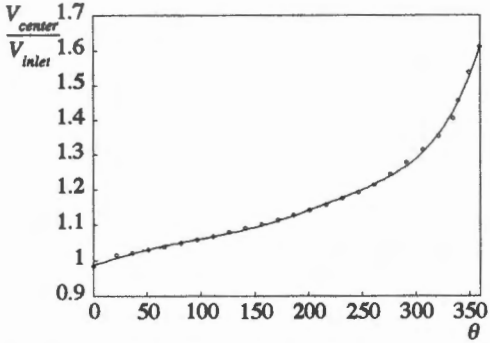

Fig. 9 Velocity distribution along center stream-line

Frictional resistance coefficient and admissible roughness

Defining the cross sectional area A_S and the perimeter S_S of the spiral case as shown in Fig. 10 at an arbitrary circumferential angle, the hydraulic mean depth m_S can be calculated as follows;

$$m_S = \frac{A_S}{S_S} \tag{13}$$

The equivalent diameter D_e of the spiral case is determined with the following equation;

$$D_e=4m_s \tag{14}$$

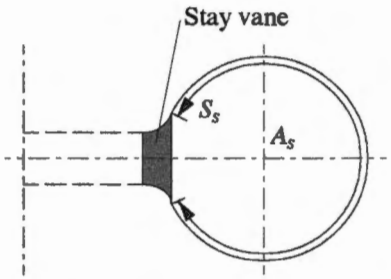

Fig. 10 Area and peripheral length of case

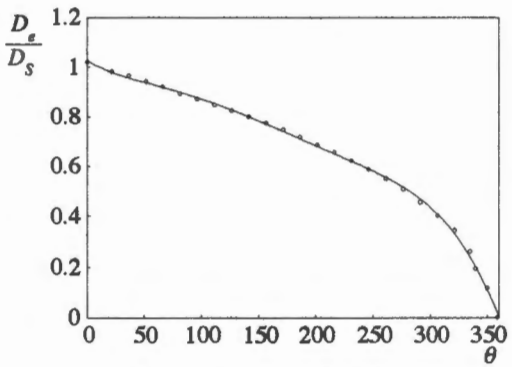

Fig. 11 Equivalent diameter vs circumferential angle

Figure 11 shows the distribution of equivalent diameter (non-dimensioned with the inlet diameter D_s) versus the circumferential angle that does not decrease linearly. The frictional resistance coefficient for the spiral case λ_s is assumed to be applied with Eq. (15) by Colebrook and White;

$$\frac{1}{\sqrt{\lambda_s}} = -2\log\left(\frac{ks/D_e}{3.71} + \frac{2.51}{Re\sqrt{\lambda_s}}\right) \tag{15}$$

where ks is the height of grain for equivalent sand roughness, and Re the Reynolds number based on the mean flow velocity and the diameter of the pipe. Since the surface roughness of the model spiral case is measured with the arithmetic mean roughness Ra, the roughness conversion coefficient C_k (= ks/Ra) is necessary.
There is a variety of values in the roughness conversion coefficient C_k[4]. Assuming C_k = 4.2 and using the Reynolds number at the case inlet as a reference Reynolds number, the frictional resistance coefficient λ_S is calculated with Eq. (15). Table 2 shows the values of Ra, ks, $\lambda_{S\text{-}inlet}$ with Eq. (15) and λ_{smooth} obtained with the universal friction formula for the smooth pipe.

Table 2 Roughness and resistance coefficient

Roughness condition	head (m)	Ra	ks	$\lambda_{S\text{-}inlet}$	λ_{smooth}
Smooth	10	0.5	2.10	0.01122	0.01110
Roughened	10	5	21.0	0.01217	0.01113
Smooth	5	0.5	2.10	0.01187	0.01178
Roughened	5	5	21.0	0.01267	0.01181

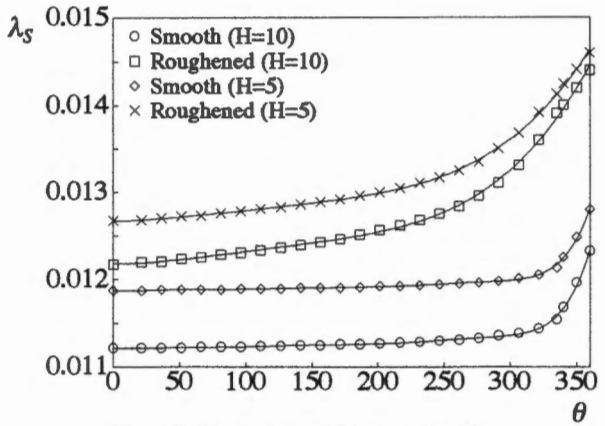

Fig. 12 Variation of frictional resistance coefficient vs circumferential angle

The value of $\lambda_{s\text{-}side}$ for the smooth case is close to λ_{smooth}. It implies that the surface roughness of 0.5 Ra is nearly admissible roughness. Since the $\lambda_{s\text{-}side}$ of roughened case is higher than λ_{smooth}, on the other hand, the roughness of 5 Ra exceeds the admissible roughness for the spiral case. The distribution of the frictional resistance coefficient for the segments of the spiral case is shown in Fig. 12. For the smooth case, the region except the spiral end is hydraulic smooth under the test head of 5 m, however, the effect of roughness may slightly appear under the test head of 10 m. On the other hand, the roughened case shows the clear effect of roughness from the start of spiral irrespective of the test heads.

Frictional deficiency in spiral case

The frictional loss in a segment of the spiral case dH_s is assumed to be calculated with the Darcy-Weisbach's Eq. (16) as follows;

$$dH_s = \lambda_s \frac{R_{center}\, d\theta}{D_e} \frac{V_{center}^{\ 2}}{2g} \tag{16}$$

where $d\theta$ is the infinitesimal circumferential angle and g the acceleration due to gravity.

The overall frictional loss head ΔH_s in the spiral case is obtained by integrating dH_s from 0 degree at the front side of the nose stay vane to the rear side.

$$\Delta H_s = \int_0^{\theta_i} dH_s = \int_0^{\theta_i} \lambda_s \frac{R_{center}}{D_e} \frac{V_{center}^{\ 2}}{2g} d\theta \tag{17}$$

The frictional deficiency in the spiral case δ_{sf} is calculated against the turbine net head H as follows;

$$\delta_{sf} = \frac{\Delta H_s}{H} \tag{18}$$

Table 3 shows the predicted frictional deficiency in the spiral case δ_{sf}. The value of the deficiency δ_{sf} amounts 0.64 % (for 10 m head) and 0.75 % (for 5 m head) in the smooth case, and 0.70 % (for 10 m head) and 0.75 % (for 5 m head) in the roughened case. These values correspond to 11 % of the turbine deficiency δ_{tc} in the smooth case, and 12 to 13 % in the roughened case.

The predicted increment of deficiency by roughening the surface roughness of the spiral case is compared with the test values in Table 4. The good agreement implies that it is pertinent to estimate the roughness conversion coefficient C_k of 4.2, as well as the admissible roughness of 0.5 Ra.

Table 3 Friction deficiency in spiral case

Head(m)	δ_{Ej} of smooth	δ_{Ej} of roughened	Inrement of deficiency
10	0.00639	0.00748	0.00108
5	0.00700	0.00754	0.00054

Table 4 Increment of deficiency by roughness

Head(m)	$\Delta\ \delta_{Ej}$ of tests	$\Delta\ \delta_{Ej}$ of calculation
10	0.0011	0.00108
5	0.0005	0.00054

Concluding remarks

The increment of frictional deficiency by roughening the spiral case can be extracted from the optimum specific hydraulic energy deficiencies of a model Francis turbine measured changing surface roughness of the spiral case. On the other hand, the frictional deficiency in the spiral case is predicted under the assumptions of the roughness conversion coefficient C_k of 4.2, as well as the admissible roughness of 0.5 Ra.

(1). The optimum energy deficiency δ_{Eo} extracted from the measured performance diagrams amounts the values of 5.7 % (for 10 m head) and 6.3 % (for 5 m head) of the test head for the model turbine with all smooth components, and 5.8 % (for 10 m head) and 6.4 % (for 5 m head) with the roughened case.

(2). The calculated frictional deficiency δ_{Rf} amounts by 0.64 % (for 10 m head) and 0.75 % (for 5 m head) in the smooth case, and by 0.70 % (for 10 m head) and 0.75 % (for 5 m head) in the roughened case. These values correspond to 11 % of the turbine deficiency δ_{Ro} in the smooth case, and 12 to 13 % in the roughened case.

(3). The predicted increment of frictional deficiency by roughening the spiral case is compared with the measured one. As a result, it is pertinent to assume the roughness conversion coefficient C_k of 4.2 as well as the admissible roughness of 0.5 Ra for the relevant spiral case.

References

1. Henry, P.; "Influence de la rugosite sur le rendoment d'n modele reduit de turbine Francis", IAHR-Tokyo(1980), pp.677-688.
2. JSME standard S008 (under the revision).
3. Han, F., Ida, T. and Kubota, T.; "Experimental Loss Analyses in High Specific-speed Hydroturbines with Adjustable Blade Runner (1st Report, Variation of Runner Shock Losses with Blade Setting Angles and Operating Conditions)", JSME(B), 58-550, (1992-6), pp.1780-1787.
4. Akaike, S.;"The effect of surface roughness on prediction of turbo machinery (2nd Report : equivalent sand diameter available for surface roughness)" ,turbo machinery,19-12,(1991-12), pp.802-806.